# YAP1 activation is associated with the progression and response to immunotherapy of non-muscle invasive bladder cancer

Seung-Woo Baek,[a,b] Jeong-Yeon Mun,[c] In-Hwan Jang,[a,b] Gi-Eun Yang,[c,d] Mi-So Jeong,[c] Seon-Kyu Kim,[b,e] Jong-Kil Nam,[f] In-Sun Chu,[a,b]* and Sun-Hee Leem[c,d]**

[a]Genome Editing Research Center, Korea Research Institute of Bioscience and Biotechnology (KRIBB), Daejeon 34141, Republic of Korea
[b]Department of Bioinformatics, KRIBB School of Bioscience, Korea University of Science and Technology, Daejeon 34113, Republic of Korea
[c]Department of Biomedical Sciences, Dong-A University, Busan 49315, Republic of Korea
[d]Department of Health Sciences, The Graduated of Dong-A University, Busan 49315, Republic of Korea
[e]Personalized Genomic Medicine Research Center, KRIBB, Daejeon 34141, Republic of Korea
[f]Department of Urology, Research Institute for Convergence of Biomedical Science and Technology, Pusan National University Yangsan Hospital, Yangsan 50612, Republic of Korea

## Summary

**Background** Despite the availability of several treatments for non-muscle-invasive bladder cancer (NMIBC), many patients are still not responsive to treatments, and the disease progresses. A new prognostic classifier can differentiate between treatment response and progression, and it could be used as a very important tool in patient decision-making regarding treatment options. In this study, we focused on the activation of Yes-associated protein 1 (*YAP1*), which is known to play a pivotal role in tumour progression and serves as a factor contributing to the mechanism of resistance to various relevant therapeutic agents. We further evaluated its potential as a novel prognostic agent.

**Methods** We identified *YAP1*-associated gene signatures based on UC3-siYAP1 cells (n=8) and NMIBC cohort (n=460). Cross-validation was performed using 5 independent bladder cancer patient cohorts (n=1006). We also experimentally validated the changes of gene expression levels representing each subgroup.

**Findings** The 976-gene signature based on *YAP1*-activation redefined three subgroups and had the benefits of Bacillus Calmette-Guérin (BCG) treatment in patients with NMIBC (hazard ratio 3.32, 95% CI 1.29-8.56, *p* = 0.01). The integrated analysis revealed that *YAP1* activation was associated with the characterization of patients with high-risk NMIBC and the response to immunotherapy.

**Interpretation** This study suggests that *YAP1* activation has an important prognostic effect on bladder cancer progression and might be useful in the selection of immunotherapy.

**Funding** A funding list that contributed to this research can be found in the Acknowledgements section.

**Keywords:** Non-muscle-invasive bladder cancer (NMIBC); *YAP1*; Prognosis; Bacillus Calmette-Guérin (BCG); Immunotherapy

*Corresponding author at: Genome Editing Research Center, Korea Research Institute of Bioscience and Biotechnology, 125 Gwahak-ro, Yuseong-gu, Daejeon 34141, Republic of Korea.
**Corresponding author at: Department of Biomedical Sciences, Dong-A University, Busan 49315, Republic of Korea.
*E-mail addresses:* chu@kribb.re.kr (I.-S. Chu), shleem@dau.ac.kr (S.-H. Leem).

## Introduction

Bladder cancer accounts for 150,000 cancer-related deaths annually.[1] Of patients with newly diagnosed bladder cancer, approximately 70 to 80% present with non-muscle-invasive bladder cancer (NMIBC), which comprises Ta tumours located in the mucosa only, T1 tumours with submucosal invasion, and carcinoma in situ (CIS) with flat and high-grade dysplasia lesions.[2]

### Research in context

*Evidence before this study*

Non-muscle invasive bladder cancer (NMIBC) is clinically heterogeneous. Many NMIBC patients do not respond to Bacillus Calmette-Guérin (BCG) immunotherapy and often experience disease progression. Improving the patient diagnosis is a major challenge, and various treatment options suggested to NMIBC patients need further development. Immune checkpoint inhibitors (ICIs) are already used for the treatment of muscle invasive bladder cancer (MIBC), but only a limited number of patients respond to treatment. YAP1 is emerging as a key gene in the response to various therapies, including ICIs. Although several predictive markers have been proposed, the underlying mechanisms controlling the response to ICIs have not been fully elucidated.

*Added value of this study*

With the gene signature associated with YAP1 activation, the benefit of BCG therapy was discovered in a subgroup of NMIBC patients, and the potential of ICIs therapy for high-risk NMIBC patients was confirmed by integrated analysis with the IMvigor210 cohort.

*Implications of all the available evidence*

The newly established classification system supports BCG and ICIs treatment options for high-risk NMIBC patients. These findings could contribute to precision medicine in NMIBC patients by classifying optimal patient subgroups and determining the appropriate course of treatment.

Approximately 10 to 20% of patients with NMIBC progress to muscle-invasive bladder cancer (MIBC).[3] As a clinical approach for patients with NMIBC, transurethral resection (TUR) followed by adjuvant intravesical therapy (IVT) with Bacillus Calmette-Guérin (BCG) is recognized as the best treatment option for patients with high-risk features.[4] However, due to the clinical heterogeneity of bladder cancer, many patients fail to respond to BCG treatment and progress to MIBC,[5] indicating that effective second-line treatment options are needed. Several immunotherapy trials are currently ongoing, and much more effort is still needed to better evaluate the oncologic outcomes of immunotherapy for patients with NMIBC.[6] Although clinical variables, such as the T stage, tumour size, and tumour grade, were identified as independent prognostic factors, the usefulness of these prognostic factors to predict patient outcomes after treatment is limited.[4] As part of precision medicine, studies performing a genome-wide analysis of bladder cancer strongly indicated that heterogeneity is well reflected in the gene expression profile, confirming that tumour heterogeneity has a molecular basis.[7-11] However, despite these efforts, the

ability to predict the response of patients with NMIBC to various treatments is still insufficient, and further analysis of a different aspect of tumour heterogeneity is required.[12]

Yes-associated protein 1 (*YAP1*) is an important oncogene whose biological activity is regulated by the Hippo pathway. When Hippo signalling is active, *MST1/2*, *SAV1*, *LATS1/2*, and *MOB1* form core complexes that inactivate *YAP1* and *TAZ* by phosphorylation; in contrast, phosphorylated *YAP1* and *TAZ* enter the nucleus and induce the transcription of genes that regulate tumorigenesis, cell growth, and the suppression of apoptosis. YAP1 is thus an important oncoprotein that plays a pivotal role in the progression of numerous tumour types.[13] Furthermore, emerging evidence indicates that *YAP1* activation may be a major mechanism underlying the resistance to various therapies.[14] Although a number of studies have been conducted on NMIBC, research on the correlation between *YAP1* activation and the prognosis of patients with NMIBC is needed.[15,16]

Here, we investigated distinct molecular subgroups stratified according to *YAP1* activation that displayed different prognoses and treatment responsiveness, and generated a gene signature that stratified patients with NMIBC into these subgroups. Using multiple patient cohorts and various experiments, we validated whether our signature showed prognostic or therapeutic relevance. The *YAP1* signature provided evidence to classify high-risk patients with NMIBC who were responsive to BCG treatment. Through an integrated analysis of the NMIBC and MIBC cohorts, we propose that a subgroup of patients with NMIBC may benefit from immune checkpoint inhibitor (ICI)-based treatment.

## Methods

### Ethics

There are no ethical issues in this study because standard cell lines and clinical cohort data of the public domain were used. All experiments were conducted in accordance with the relevant regulations and guidelines.

### Patient cohorts and gene expression profile data

A breast epithelial cell line (MCF10A) and 30 bladder cancer cell lines were used in a preliminary study to select the appropriate bladder cancer cell lines (GSE70506, n=6; GSE97768, n=30).[10,17] The URO-MOL cohort was used as a discovery dataset and to refine the prognostic gene expression signature (E-MTAB-4321; n=460).[8] The Korean (GSE13507, n=165)[18] and Lund cohorts (GSE32894, n=308)[7] were used for the validation dataset. For characterization, Yonsei (GSE120736, n=145),[9] TCGA (n=407),[10] and IMvigor210 (n=298) cohorts[19] were used. All of the gene

expression data and clinical information are available in the Gene Expression Omnibus (GEO) database from NCBI, the European Bioinformatics Institute (EBI) Array Expression database, the IMvigor210CoreBiologies R package,[19] and the Cancer Browser (https://xenabrowser.net). The clinical characteristics of patients with bladder cancer in six independent cohorts are described (Supplementary Table 1). For RNA-seq data, the read counts per million fragments mapped (CPM) of each sample were used to estimate the expression level of each gene. All gene expression data were separately log2 transformed and quantile normalized. We illustrate a schematic workflow for the bioinformatics analysis (Supplementary Figure 1).

### RNA isolation and RNA-seq data processing

RNA samples for sequencing were isolated using the Qiagen RNeasy Mini Kit (Qiagen, Hilden, Germany) according to the manufacturer's protocol. Total RNA was subjected to a reverse transcription reaction with poly (dT) primers using PrimeScript[TM] reverse transcriptase (Takara, Shiga, Japan) according to the manufacturer's protocol. The library quality and quantity were measured using a Nanodrop spectrophotometer (ND-1000; Thermo Scientific, MA, USA). Paired-end reads were sequenced using the NovaSeq-6000 platform (Illumina, CA, USA). Reference genome sequence data from *Homo sapiens* were obtained from the Ensemble genome browser (assembly ID: GRCh38). Reference genome indexing and read mapping of samples were performed using STAR software (ver. 2.6.1a).[20] Feature-Counts (ver. 1.6.2) software was then used to calculate the generated binary alignment map files.[21] The RNA-seq dataset generated in this study is available in the GEO public database under data series accession number GSE186043.

### Cell culture

The human bladder cancer cell lines RT4 (Cat#30002, RRID: CVCL_0036, Korea Cell Line Bank, Seoul, Korea), T24 (Cat#30004, RRID: CVCL_0554, American Type Culture Collection, MD, USA), UM-UC-3 (UC3; #CRL_1749, RRID: CVCL_1783, American Type Culture Collection, MD, USA), and UM-UC-14 (UC14; Cat#08090509, RRID: CVCL_2747, European Collection of Authenticated Cell Cultures, UK) were purchased. RT4, T24, and UC14 cell lines were cultured in DMEM supplemented with 10% FBS and 1% penicillin/streptomycin (Cat# FBS, Cat# PS-B, Capricorn Scientific GmbH, Ebsdorfergrund, Germany), while the UC3 cell line was cultured in MEM (Cat# LM007-54, WELGENE, Korea) supplemented with 10% FBS and 1% penicillin/streptomycin at 37 °C with 5% $CO_2$. These cells were validated by the results of a short tandem repeat (STR) DNA profiling assay, cytochrome C oxidase I assay, and mycoplasma contamination assay.

### Vectors and small interfering RNA

For *YAP1* overexpression experiments, RT4 and UC14 cell lines were transiently transfected with the YAP1-S127A mutant vector and empty vector from Asan Medical Center (Seoul, Korea). For *YAP1* knockdown experiments, T24 and UC3 cell lines were transiently transfected with siYAP#1 and siYAP#2 purchased commercially (Integrated DNA Technologies, LA, USA) and a scrambled siRNA control (scRNA).

### Generation of stable cell lines

The shYAP1-expressing plasmid (RRID: Addgene_27368) and lentiviral packaging plasmids pMD2.G (RRID: Addgene_12259, Addgene, MA, USA) and psPAX2 (RRID: Addgene_12260, Addgene, MA, USA) were purchased. We used a pLKO.1-puro nontarget shRNA plasmid (Cat#SHC016, Sigma−Aldrich, MO, USA) as the negative control. The shRNA-expressing plasmid (shNTS or shYAP1), pMD2.G, and psPAX2 plasmids were cotransfected into the HEK-293T cell line using jetPRIME reagent (Cat# 101000053, Polyplus-transfection Inc., NY, USA). We replaced the medium with fresh medium containing antibiotics after 12 h. Polybrene was added to the supernatant, and medium containing lentiviral particles was used to transduce the UC3 cell line. Puromycin (5 μg/ml, Cat# 9620, Sigma−Aldrich, MO, USA) was used to select cells stably expressing the shRNA against NTS (shNTS) or *YAP1* (shYAP1). *YAP1* mRNA and protein levels in cell lines were confirmed using qRT−PCR and Western blot analysis, respectively.

### Quantitative real-time polymerase chain reaction (qRT−PCR)

Total RNA was isolated using RNAiso Plus (Cat# 9108, Takara, Shiga, Japan). All primers were designed and are listed in Supplementary Table 2. The cDNA templates were synthesized using the PrimeScript[TM] RT reagent kit (Cat# RR036A, Takara, Shiga, Japan). Using the obtained cDNAs as templates, qPCR was performed using SYBR Premix Ex Taq (Tli RNaseH Plus, Cat# RR420, Takara, Shiga, Japan) and CFX96[TM] Optical Reaction Module (Cat# 184-5096, Bio−Rad, CA, USA). The data were analysed using CFX Manager[TM] (Bio−Rad, CA, USA).

### Western blot analysis and antibodies

Cells were collected after washes with PBS, lysed in 100 μL of radioimmunoprecipitation (RIPA) buffer containing protease inhibitors (Cat# 04693116001, Roche, Mannheim, Germany) and sonicated. Protein

concentrations were determined using the Pierce™ BCA Protein Assay kit (Cat# 23227, Thermo Fisher Scientific, IL, USA). Primary antibodies against GAPDH (Cat# 2118, RRID: AB_561053, Cell Signaling Technology, MA, USA), YAP1 (Cat# 4912, RRID: AB_2218911, Cell Signaling Technology, MA, USA), p-YAP1 (S127) (Cat# 4911, RRID: AB_2218913, Cell Signaling Technology, MA, USA), CYR61 (Cat# sc-374129, RRID: AB_10947399, Santa Cruz Biotechnology, CA, USA), CCNA2 (Cat# NBP1-31330, RRID: AB_10003781, Novus Biologicals, CO, USA), E2F1 (Cat# A300-766A, RRID: AB_2096774, Bethyl Laboratories, TX, USA), and FOXM1 (Cat# A301-533A, RRID: AB_999586, Bethyl Laboratories, TX, USA) were used.

### Clonogenic assay

The ability to form colonies was confirmed by performing a clonogenic assay. shNTS- and shYAP1-transfected cells were inoculated into 12-well plates at a density of $5 \times 10^2$ cells/well. After an incubation for 6 days, colonies were formed, stained with 0.05% crystal violet (Cat# C3886, Sigma−Aldrich, MO, USA) and counted using the ImageJ program from the National Institutes of Health.

### MTT assay

Cell viability was measured using the MTT assay. A total of 2000 cells/well were seeded in 96-well plates, and cells were incubated for 0, 24, and 48 h. Then, 10 μL of MTT (5 mg/ml; Sigma−Aldrich, MO, USA) were added to each well and incubated for 1 h. After the incubation, the supernatant was removed, 100 μL of dimethyl sulfoxide (DMSO; Cat#D1370, Duchefa, Amsterdam, Netherlands) were added to each well, and the absorbance was measured at 540 nm using a Wallac Victor 1420 Multilabel Counter (PerkinElmer Inc., MA, USA).

### Invasion and migration assays

Cell invasion and migration were confirmed using a standard 48-well chemotactic chamber (Cat#AP48, Neurolob Lobe, MD, USA). A membrane with a pore size of 8 μm was precoated with Matrigel (Cat# 354234, Corning, MA, USA) and collagen (Cat# C7661, Sigma−Aldrich, MO, USA). Thirty microliters of medium containing 1% FBS were dispensed in the bottom chamber. Cells were suspended in FBS-free medium and seeded at a density of $1 \times 10^4$ cells/56 μL in the top chamber. After an incubation for 24 h, the membrane was stained with Diff Quik reagent (Cat#38721, Sysmex, Kobe, Japan). Migrated and invaded cells were observed under a microscope (Axiovert 40 CFL; Carl Zeiss, Oberkochen, Germany).

### Statistical analysis

ConsensusClusterPlus (ver. 1.52.0) and K-means clustering algorithms were used for transcriptional profiling of patients with bladder cancer and to determine the appropriate number of clusters.[22] The expression levels of each gene in each dataset were independently standardized to a mean of zero and a standard deviation of 1 to integrate and analyse gene expression profiles obtained from different platforms. K-means clustering analysis was conducted using Gene Cluster 3.0 and visualized using TreeView™. Gene Ontology (GO) enrichment analysis was performed using the Database for Annotation, Visualization, and Integrated Discovery (DAVID) tool (https://david.ncifcrf.gov) with significance criteria (FDR < 0.25) to explore significantly enriched functions. Kaplan−Meier plots were constructed to estimate associations between subgroups and survival outcomes using the log-rank test. The comparisons of objective responses were estimated using Fisher's exact test. All statistical analyses were performed in the R 4.0.2 language environment (https://www.r-project.org).

### Role of the funding source

The funders had no role in the study design, data collection and analysis, decision to publish, or preparation of the manuscript.

## Results

### Screening of bladder cancer cell lines for analysis and validation

YAP1 in the Hippo pathway is a particularly well-known oncogene, but studies of YAP1 in bladder cancer are still lacking. In this study, we analysed RNA-seq data in the MCF10A breast epithelial cell line[17] and selected 2,151 genes associated with YAP1 overexpression ($p < 0.001$ and 2-fold change). Using these genes, hierarchical clustering analysis was applied by merging data from MCF10A and bladder cancer cell lines.[10] MCF10A cells were included in each of the two subgroups of bladder cancer cell lines stratified according to YAP1 overexpression (Figure 1a). The relative expression levels of five genes associated with YAP1 activation (YAP1, CYR61, CTGF, and TEAD2)[13] and FGFR3, which is associated with tumour heterogeneity,[23] were analysed in four cell lines whose phenotype was defined as control-like BC (control-like bladder cancer cell lines; RT4 and UC14) and YAP1 OE-like BC (YAP1 overexpression-like bladder cancer cell lines; UC3 and T24) for further experimental study (Figure 1a and 1b).[24] Based on the RT4 cell line, which is most similar to the breast epithelial cell line, the expression of the YAP1, CYR61, CTGF, and TEAD2 genes increased in the UC14, T24, and UC3 cell lines. The expression of the FGFR3 gene was also significantly decreased in the UC14, T24, and UC3 cell lines (Figure 1c). When transfected with YAP1-S127A, the expression levels of CYR61, CTGF, and TEAD2 were
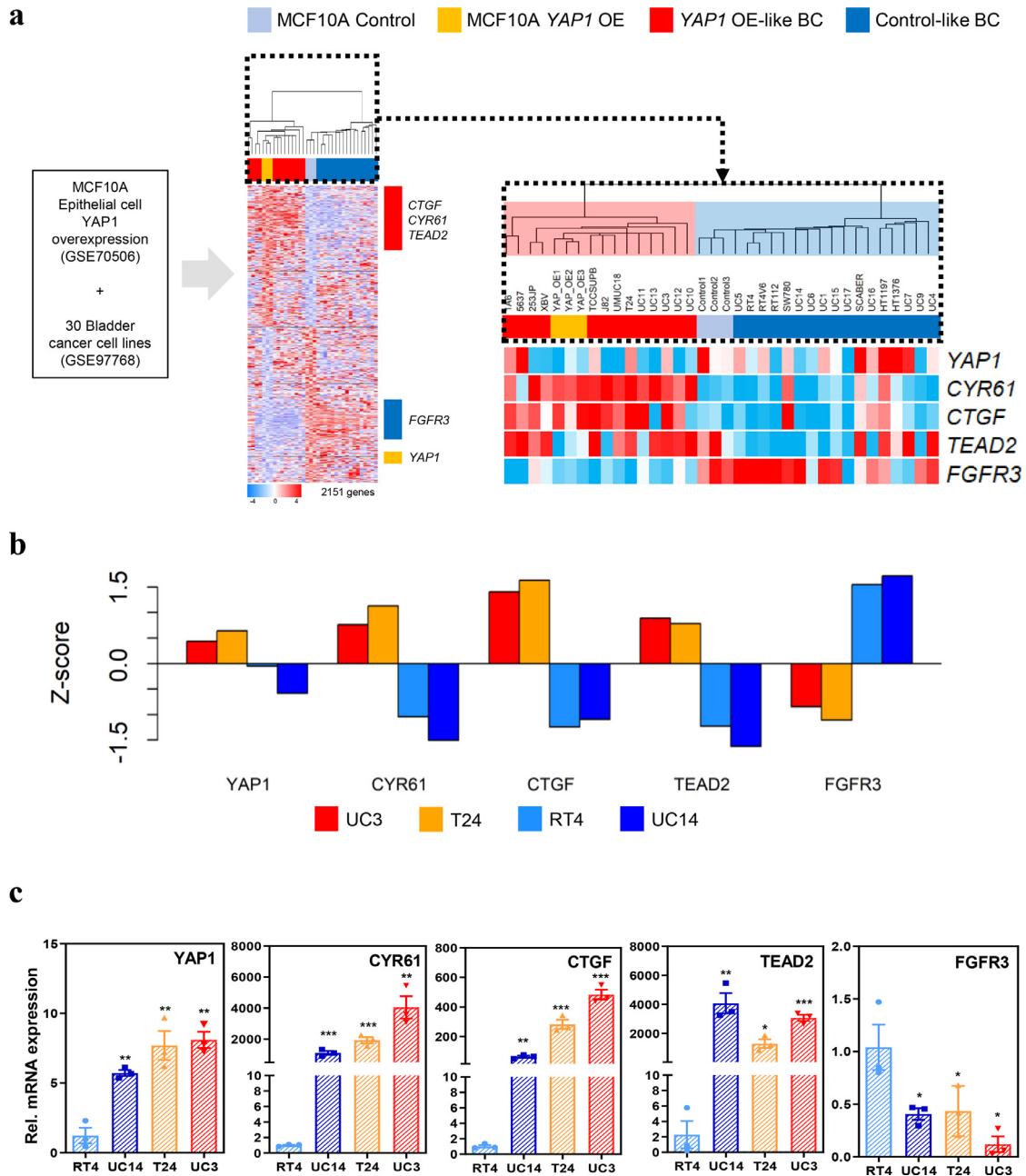
**Figure 1.** Clustering analysis of integrated gene expression data after *YAP1* overexpression in both breast epithelial cell and bladder cancer cell lines (GSE70506 and GSE97768). (a) A heatmap providing an overview of the unsupervised hierarchical cluster analysis of gene expression data from 36 samples (3 epithelial cells, 3 epithelial cells with *YAP1* overexpression, and 30 bladder cancer cell lines). Genes whose expression was significantly ($p < 0.001$ and 1·5-fold changes) associated with overexpression of *YAP1* in the MCF10A cell line were only used for clustering. Each cell in the matrix represents the expression level of a gene feature in an individual sample. Red and blue cells reflect high and low expression levels, respectively. The genes captured represent those that were differentially expressed between the *YAP1* overexpression-like bladder cancer cell (*YAP1* OE-like BC) and control-like bladder cancer cell (Control-like BC) subgroups. (b) Comparison of the 5 genes expression levels in 4 bladder cancer cells representing the *YAP1* OE-like BC and Control-like BC subgroups. (c) The mRNA levels of genes downstream of *YAP1*, namely, *CYR61*, *CTGF*, *TEAD2,* and *FGFR3* were confirmed in four bladder cancer cell lines using qRT−PCR. The data are presented as the means ± standard deviations of three independent experiments. *, $p < 0.05$; **, $p < 0.01$; and ***, $p < 0.001$.

increased, and *FGFR3* expression was decreased in the RT4 and UC14 cell lines (Supplementary Figure 2a). The expression levels of *CYR61, CTGF,* and *TEAD2* were significantly decreased, and *FGFR3* expression was increased in the UC3 and T24 cell lines transfected with siYAP1 (Supplementary Figure 2b). In addition, protein levels of YAP1 and its downstream factor CYR61 were confirmed in four cell lines, and both proteins showed the highest expression in the UC3 cell line (Supplementary Figure 2c). Based on these results, the UC3 cell line was suitable for further experiments to identify a trend in the expression of downstream genes with *YAP1* expression.

### Separation of patients with NMIBC into subgroups according to YAP1 activation

We newly generated RNA-seq data from the UC3 bladder cancer cell line transfected with siYAP1 to identify differentially expressed genes associated with *YAP1* inactivation ($p < 0.01$, 1·5-fold change, Supplementary Figure 3a). Genes involved in *YAP1* inactivation, such as *YAP1-* and *TAZ*-stimulated gene expression, were enriched ($p < 0.05$ and FDR $< 0.25$, Supplementary Figure 3b). Among the 549 differentially expressed genes, the 50 genes with the most significant differences in expression were selected ($p < 0.001$, 2-fold change; Supplementary Table 3). These genes were combined with data from the UROMOL cohort, and K-means clustering analysis was performed to discover subgroups in the cohort. siYAP1-transfected cells and *YAP1*-inactivated patients were closely coclustered, while siCon-transfected cells and *YAP1*-activated patients were closely coclustered (referred to as the *YAP1*-activated or YA subgroup and as the *YAP1*-inactivated or YI subgroup). However, the 50 genes only reflect *YAP1* activation under cellular experimental conditions, not the biological characteristics associated with patients with NMIBC. Therefore, a two-sample t test was used with a stringent threshold cutoff to evaluate gene expression data from the UROMOL cohort and identify genes significantly related to *YAP1* activation. This approach identified 976 genes that were differentially expressed between the YA and YI subgroups of patients with NMIBC in the UROMOL cohort ($p < 0.001$ and 1·5-fold change, Supplementary Figure 3c and Supplementary Table 4).

With the 976-gene signature, the consensus clustering method was used to determine the optimal number of subgroups that would distinguish patients with NMIBC, and the gene expression data were more reasonable when dividing patients into three groups (Supplementary Figure 4a). By applying consensus clustering analysis, three major clusters were observed: the YA1, YA2, and YI subgroups (Supplementary Figure 4b). The expression of well-known downstream targets of *YAP1*, such as *TEAD2, CTGF*, and *CYR61*, was significantly elevated in the YA1 and YA2 subgroups (Supplementary Figure 4c). GO analysis using the DAVID tool was applied to each subgroup-specific gene to identify the biological characteristics. When analysing YA1-specific genes, those involved in cell division, the G1/S transition of the mitotic cell cycle, and DNA repair were significantly enriched. In the analysis of YA2-specific genes, those involved in cell adhesion, immune response, chemotaxis, and angiogenesis were significantly enriched. YI-specific genes involved in embryonic skeletal system morphogenesis and anterior/posterior pattern specification were enriched (Supplementary Figure 4d).

### YAP1 activation is significantly associated with progression-free survival and the benefit of intravesical therapy (IVT) in patients with NMIBC

Among the active signalling pathways identified in each subgroup, 32 genes were derived from the 976-gene signature for an efficient analysis (Figure 2a). The 7 genes (*GATA2, GATA3, SMAD3, SMAD6, SMAD9, SHH,* and *FGFR3*) that showed an association with the YI subgroup had characteristics of the luminal papillary. The 10 genes (*BIRC5, BRCA1, BRCA2, AURKA, AURKB, FOXM1, E2F1, E2F2, CCNA2,* and *LMNB1*) that showed associations with the YA1 subgroup were involved in the DNA damage and repair (DDR) pathway. The 6 genes (*TEAD2, CTGF, CYR61, CXCL9, CXCL10,* and *CXCL11*) that showed associations with both the YA1 and YA2 subgroups were involved in *YAP1* downstream regulation and immune infiltration, respectively. The 9 genes (*PDGFRA, VIM, ZEB1, ZEB2, CXCL12, NEGR1, ACTA2, TAGLN,* and *TCF4*) that showed associations with the YA2 subgroup were involved in epithelial-mesenchymal transition (EMT) and TGFβ pathway activation. Through an analysis of the clinical characteristics related to the three subgroups, many high-risk patients with bladder cancer, such as T1 stage and high grade, were included in the YA1 subgroup. Additionally, class 2 of the UROMOL cohort was subdivided into the YA1 and YA2 subgroups (Figure 2a). The progression rate of the YA1 subgroup was significantly higher than that of the YA2 and YI subgroups (log-rank test, $p < 0.001$, Figure 2b). Cox regression analysis was applied to determine the prognostic independence of the signature. In the multivariate analysis, the significant prognostic indicators of progression-free survival in subgroup YA1 included stage and grade, along with the 976-gene signature in the UROMOL cohort (hazard ratio 3·32, 95% CI 1·29-8·56, $p = 0.01$; Supplementary Table 5). Importantly, IVT considerably affected progression-free survival in the patients within the YA1 subgroup (log-rank test, $p = 0.05$, Figure 2c), whereas no significant association between IVT and the YA2 or YI subgroups was observed (log-rank test, $p = 0.4$ and $p = 0.99$, Figure 2d and e). These results reveal the predictive ability of the
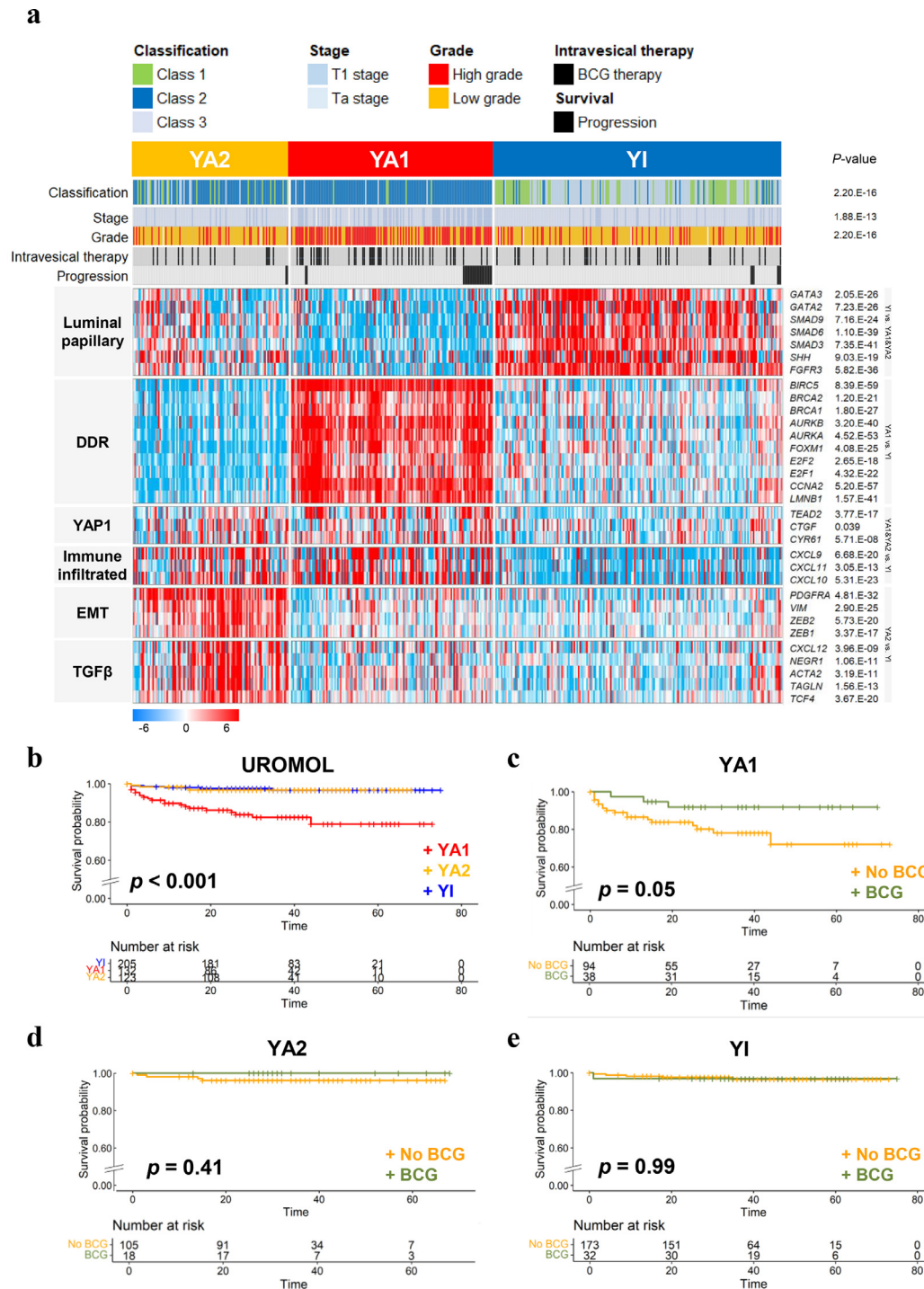
**Figure 2.** Transcriptional profiling of 32 genes in patients with NMIBC from the UROMOL cohort. Analysis of the associations between *YAP1* activation 1 (YA1), *YAP1* activation 2 (YA2), and *YAP1* inactivation (YI) subgroups, core biological pathways, and progression-free survival. (a) Heatmap of the clinical and biological features of patients with NMIBC in the UROMOL cohort. Rows in the heatmap show gene expression grouped by associated biological pathways. The colours in the heatmap reflect relatively high (red) and low (blue) expression (Z score) levels. *P value*s in the classification, stage, and grade were obtained using the chi-square test. *P value*s for gene expression were obtained using a two-sample t test. (b) Progression-free survival of the UROMOL cohort ($p < 0.001$ using the log-rank test). (c-e) Progression-free survival of the YA1, YA2, and YI subgroups ($p = 0.05$, $p = 0.40$, and $p = 0.99$ using the log-rank test). Data were plotted according to whether patients received intravesical treatment (BCG). DDR, DNA replication and DNA damage response; EMT, epithelial-mesenchymal transition; BCG, Bacillus Calmette-Guérin.

signature defined by *YAP1* activation in classifying high-risk patients with NMIBC who might benefit from BCG-based immunotherapy.

### Independent validation and characterization of the prognostic value of YAP1 activation in bladder cancers

A cohort was created by combining the gene expression profile and clinical data from patients with NMIBC in the Lund and Korean cohorts to validate the association between *YAP1* activation and patient prognosis. Consistent with previous results from the UROMOL cohort, most high-risk patients with NMIBC were included in the YA1 and YA2 subgroups (Supplementary Figure 5a). Our previous study presented two subtypes of NMIBC, the high *CCNB1* cluster (HC) and the low *CCNB1* cluster (LC), as a result of tumour heterogeneity defined by the *CCNB1* signature.[11] The HC of the *CCNB1* cluster was subdivided into YA1 and YA2 subgroups (Supplementary Figure 5a). The ratio of NMIBC progression in patients within the YA1 and YA2 subgroups was significantly higher than that in patients within the YI subgroup (Supplementary Figure 5b). In the multivariate analysis, the significant prognostic indicators of progression-free survival in the YA1 subgroup included stage and grade along with the 976-gene signature (hazard ratio 4·65, 95% CI 1·61-13·4, *p* < 0·001; Supplementary Table 5).

In addition, multiple cohorts (the Lund, Korean, and Yonsei cohorts), including patients with NMIBC and MIBC, were analysed according to the 976-gene signature to determine the association between *YAP1* activation and the prognosis (Supplementary Figures 6a, 7a, and 8a). As expected, a significantly higher rate of disease progression was observed in patients within the YA1 and YA2 subgroups than in those within the YI subgroup (Supplementary Figures 6b and 7b), and most high-risk patients with NMIBC were included in the YA1 and YA2 subgroups (Supplementary Figures 6c, 7c and 8b). Thus, the 976-gene signature produces consistent outcomes for cohorts of both patients with NMIBC and MIBC.

### Experimental validation of YAP1 activation

*YAP1* knockdown experiments were performed to investigate its effect on the proliferation and motility of the UC3 cell line and to verify the results in vitro. Using two types of siRNAs, siYAP1#1 and siYAP1#2, cells with over 70% reductions in *YAP1* mRNA and protein levels were generated (Supplementary Figure 9a). As expected, reduced cell viability, colony formation, invasiveness, and migration was observed in siYAP1-transfected cells compared to those transfected with the scRNA (Supplementary Figure 9b-d). The expression levels of *CCNA2, TEAD2, CTGF, CYR61, SMAD3, and SMAD6* were altered in the UC3 cell line

(Supplementary Figure 9e). Additionally, CTGF, CYR61, and CCNA2 protein levels were reduced (Supplementary Figure 9f). Based on these results, we thought that a reasonable approach would be to observe phenotypic shifts and gene expression levels under stable conditions. Using the UC3 cell line stably transfected with shRNA-*YAP1* (shYAP1), a cell line with reduced mRNA and protein expression levels of *YAP1* was generated (Figure 3a). As expected, reduced cell viability, colony formation, invasiveness, and migration was observed in shYAP1-expressing cells compared to shNTS-expressing cells (Figure 3b and 3c). The results showed that the gene expression levels associated with the YA1 and YA2 subgroups were decreased, whereas the gene expression level associated with the YI subgroup was increased in the shYAP1 group (Figure 3d). Additionally, levels of the CTGF, CYR61, E2F1, and FOXM1 proteins were reduced (Figure 3e). After transfecting the *YAP1* vector into shYAP1 cells, the expression of subgroup-related genes was restored (Figure 3f). These results suggest that *YAP1* knockdown inhibited the proliferation and migration of bladder cancer cells and was associated with the expression of genes associated with the YA1 and YA2 subgroups.

### Integrated analysis of the association with the response to immunotherapy

An integrated analysis of the IMvigor210 cohort and the UROMOL cohort based on the 976-gene signature was performed to determine how *YAP1* activation affected the response to immunotherapy (Supplementary Figure 10). The previous analysis of the gene expression profile was consistent based on 32 selected genes representing each subgroup (Figure 4a). We performed a survival analysis and estimated the prognostic value using a log-rank test to investigate the prognostic effect on the three subgroups. As a result, patients in the YA1 subgroups experienced prolonged survival after treatment with a PD-L1 inhibitor (Figure 4b). When the objective response rate (ORR) was compared among these subgroups, the YA1 subgroup exhibited a higher response rate than the other subgroups (chi-square test, *p* < 0·001, Figure 4c). When using the hazard ratio of the response to analyse the interaction between the subgroups and drug treatments, the interaction of the 976-gene signature reached a significant level in the YA1 subgroup for immunotherapy (hazard ratio 0·66, 95% CI 0·46-0·96, *p* = 0·02; Supplementary Table 6).

The PD-L1 protein was expressed at relatively high levels in immune and tumour cells in the YA1 subgroup (Supplementary Figure 11a and 11b). The tumour mutation burden (TMB) was significantly different between the YA1 and YI subgroups (Supplementary Figure 11c). Regarding TCGA classification, most of the luminal, basal, and neuronal subtypes were included in the YA1 subgroup, the luminal infiltrated subtype was included
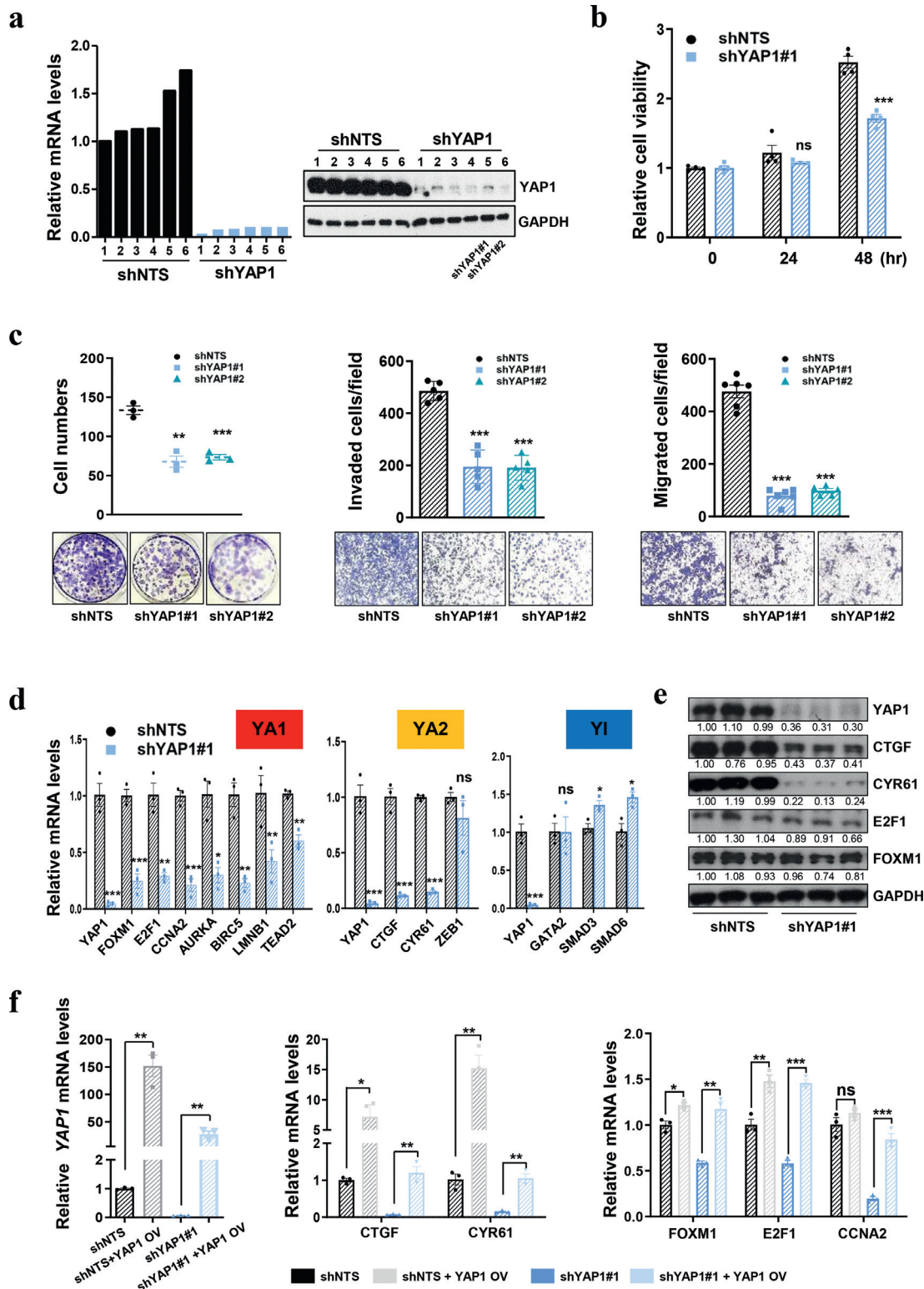
**Figure 3.** *YAP1* knockdown inhibits the proliferation of bladder cancer cells in vitro. The expression of *YAP1* subgroup target genes was partially restored by *YAP1* expression. (a) UC3 cells were infected with lentivirus expressing shYAP1 or scrambled shRNA (scRNA). *YAP1* mRNA and protein levels were detected using qRT−PCR and Western blotting, respectively. (b) Cell viability was

in the YA2 subgroup, and luminal papillary subtypes were included in the YI subgroup (Supplementary Figure 11d). In the Lund classification, the genomically unstable (GU) subtype was evenly distributed, the basal/SCC-like and urobasal B subtypes were included in the YA1 subgroup, the infiltrated subtype was included in the YA2 subgroup, and the urobasal A subtype was included in the YI subgroup (Supplementary Figure 11e). Class 2 of the UROMOL cohort was divided into the YA1 and YA2 subgroups, and classes 1 and 3 of the UROMOL cohort were included in the YI subgroup (Supplementary Figure 11f). Additionally, most high-risk patients with NMIBC were included in the YA1 subgroup (Supplementary Figure 11g and 11h). Using the 976-gene signature, an integrated analysis with TCGA and UROMOL cohorts was performed to determine how *YAP1* activation affected the prognosis of patients with MIBC. Analyses of gene expression profiles and survival were consistent across 32 selected genes representing each subgroup (data not shown). These results indicate the predictive value of the 976-gene signature for classifying both patients with MIBC and NMIBC responding to immunotherapy.

## Discussion

NMIBC is clinically heterogeneous and frequently exhibits progression to an aggressive phenotype. A previous study presented various subtypes of NMIBC, such as the UROMOL classification and the *CCNB1* cluster, as a result of tumour heterogeneity.[8,11] Despite considerable efforts to elucidate the molecular characteristics and establish prognostic models of patients with NMIBC, a study proposing various treatment decisions for precision medicine to treat patients with NMIBC, particularly focusing on *YAP1*, remains a major clinical challenge. In our previous study, *YAP1* activation was significantly correlated with heterogeneity in patients with advanced bladder cancer and was also closely related to the response to immunotherapy.[25] Experiments related to the expression of *YAP1* in bladder cancer cells showed that the efficiency of *YAP1* knockdown in the UC3 cell line was higher than that in other cell lines, and the reduction in the expression of

downstream genes was significant (Figure 1). Therefore, new transcriptomic data for UC3-siYAP1 cells were generated to observe changes in downstream genes in a bladder cancer cell line. From the combined analysis of UC3-siYAP1 and the UROMOL cohort, a 976-gene signature was identified considering the activation of *YAP1* and heterogeneity of tumours that showed a distinct prognostic difference in three subgroups of patients with NMIBC (YA1, YA2, and YI; Supplementary Figures 3 and 4).

Important biological characteristics of the YA1 subgroup are the activation of DDR-related genes (*BIRC5, BRCA1, BRCA2, AURKA, AURKB, FOXM1, E2F2, E2F1, CCNA2,* and *LMNB1*) and the large number of high-risk patients with NMIBC. Briefly, the YA1 subgroup was strongly correlated with the response to immunotherapy, such as BCG (Figure 2c) and ICIs, and exhibited better survival rates than the other subgroups (Figure 4b). The tumour DNA replication and repair landscape clearly has an important role in driving the response to ICIs.[26] The activation of EMT and TGFβ pathway activation-related genes (*PDGFRA, VIM, ZEB1, ZEB2, CXCL12, NEGR1, ACTA2, TAGLN,* and *TCF4*) are significant biological characteristics of the YA2 subgroups. Overexpression of *YAP1* in epithelial cells suppressed TGFβ1-induced apoptosis, which shifted the cellular response predominantly toward the EMT and contributed to cancer invasion and migration.[27,28] Furthermore, the EMT provides an explanation for whether diverse cancer phenotypes are promoted, and these characteristics are important causes of varying treatment outcomes.[29] The overexpression of PDGFs and PDGFRs, as well as the oncogenic alterations in these receptors, has been implicated in human cancers and is significantly correlated with poor outcomes.[30] These biological properties have been identified as a therapeutic target in the YA2 subgroup.[31,32] In addition, the YA2 subgroup exhibited a relatively poor prognosis compared with other subgroups in the integrated cohort. The biological characteristic of the YI subgroup is the activation of luminal papillary-related genes (*GATA2, GATA3, SMAD9, SMAD6, SHH,* and *FGFR3*). Typically, the *FGFR3* gene is a target for drug therapy in patients with MIBC. In

---

analysed at 0, 24, and 48 h with the MTT assay to determine the proliferation of the UC3 cell line. The data are presented as the means ± standard deviations of three independent experiments. (c) A clonogenic assay was performed with control and *YAP1* knockdown UC3 cells. Cells were stained with a crystal violet solution, and colonies were counted in three independent experiments. Invasion and migration assays of UC3 cells transfected with shNTS and shYAP1 for 24 h were performed using Boyden chamber assays. Data are presented as the means ± standard deviations of three independent experiments. (d) The *YAP1* activation 1 (YA1) genes *FOXM1, E2F1, CCNA2, AURKA, BIRC5, LMNB1,* and *TEAD2* were validated at the mRNA level after *YAP1* knockdown in the UC3 cell line. The mRNA levels of *CTGF, CYR61,* and *ZEB1* included in *YAP1* activation 2 (YA2) group were verified using qRT−PCR. The *YAP1* inactivation (YI) genes *GATA2, SMAD3,* and *SMAD6* were validated in *YAP1* knockdown cells using qRT−PCR. The data are presented as the means ± standard deviations of three independent experiments. (e) Levels of the YAP1, CTGF, CYR61, E2F1, and FOXM1 proteins were detected using Western blotting. (f) In qRT−PCR experiments, the levels of YA1 and YA2 subgroup genes were detected following *YAP1* overexpression, and the levels of YA1 and YA2 subgroup genes were restored by *YAP1* overexpression. This experiment was performed three times. *ns*, not significant; *, $p < 0.05$; **, $p < 0.01$; and ***, $p < 0.001$.
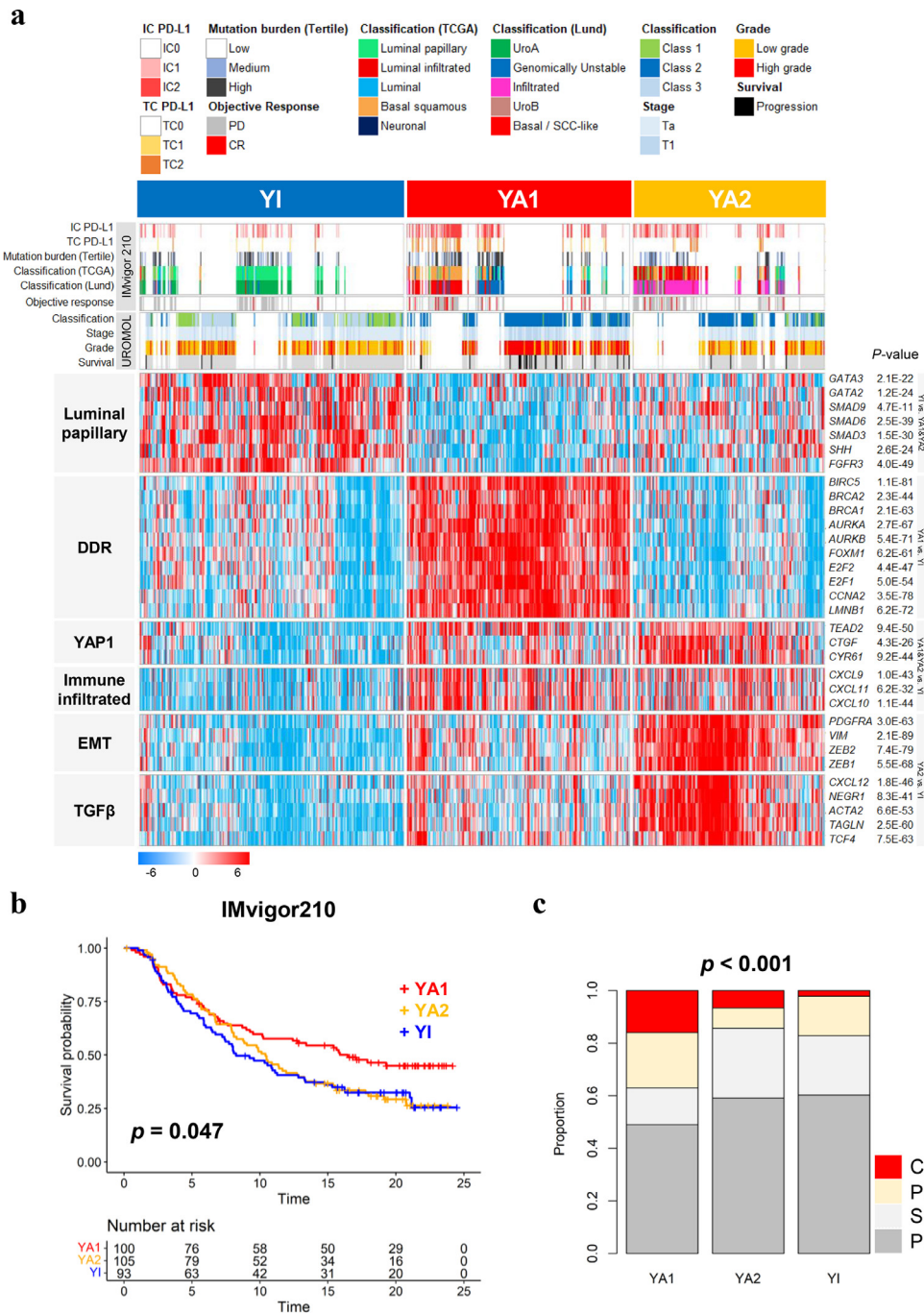
**Figure 4.** Integrated transcriptional profiling of 32 genes in patients within the merged cohort (UROMOL and IMvigor210 cohort, n=758). Associations between YA1, YA2, and YI subgroups, core biological pathways, cancer-specific survival, and objective response to immunotherapy. (a) Heatmap of the clinical and biological features of the integrated cohort. Rows of the heatmap show gene expression levels grouped by associated biological pathways. The colours in the heatmap reflect relatively high (red) and low (blue) expression (Z score) levels. *P values* for gene expression were obtained using a two-sample t test. (b) Overall survival in the IMvigor210 cohort (p = 0·04 by the log-rank test). (c) The objective response rate to immunotherapy was stratified into the three subgroups (p < 0·001 using the chi-square test). IC PD-L1, PD-L1 protein expression on immune cells; TC PD-L1, PD-L1 protein expression on tumour cells; DDR, DNA replication and DNA damage response; PD, progressive disease; SD, stable disease; PR, partial response; CR, complete response.
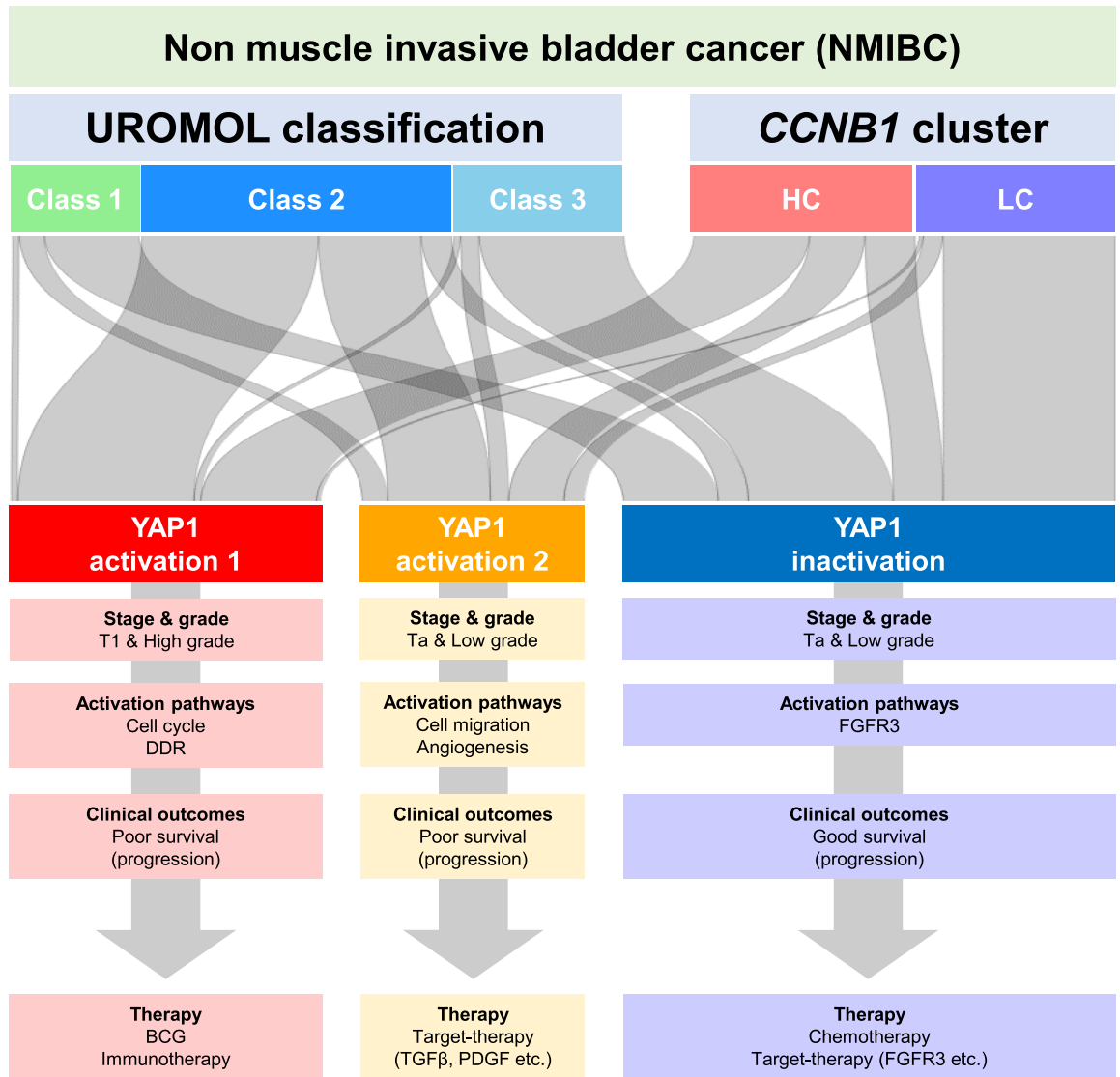
**Figure 5.** Schematic diagram of the characteristics of patients with NMIBC. Clinical and biological characteristics related to subgroups were mentioned, and suggestions for therapeutic options with potential benefits were listed. DDR, DNA replication and DNA damage response; BCG, Bacillus Calmette-Guérin.

patients with NMIBC, the prognosis is not as severe as that in patients with MIBC, but studies have suggested that activation or alteration of the *FGFR3* gene is a potential cause for progression to MIBC.[33,34] Therefore, shYAP1 experiments in the UC3 cell line were performed to verify the expression levels of representative proteins and genes (*BRCA1, AURKA, FOXM1, CCNA2, CTGF, CYR61*, and *TEAD2*) of each subgroup identified by the 976-gene signature (Figure 3). Interestingly, class 2 of the UROMOL cohort and HC of the *CCNB1* cluster were reconstructed into the YA1 and YA2 subgroups, and most of classes 1 and 3 of the UROMOL cohort and LC of the *CCNB1* cluster were reconstructed into the YI subgroup.

Taken together, the integrated analysis showed the therapeutic relevance of immunotherapy, such as BCG and ICIs, in patients within the YA1 subgroup, and a relative benefit was predicted for patients within the YI subgroup treated with standard chemotherapy and *FGFR3*-targeted therapy. In addition, targeted therapy, such as the TGFβ pathway and *PDGFRA* gene, was likely to be more advantageous for patients in the YA2 subgroup (Figure 5). Despite the conclusions regarding the prognostic effect, we also highlight the limitations of the study. Most of the studies have investigated NMIBC and MIBC separately, but our previous study investigated both bladder cancers together.[9] Therefore, a similar idea was applied in this study, and our results

provided only indirect evidence for the possibility of therapeutic drugs through an integrated analysis.

In conclusion, we suggest that three new prognostic subgroups of NMIBC reflect *YAP1* activation and exhibit significant differences in the progression of patients. Our investigations provide additional insights into the biological determinants of the response to various treatments after transurethral resection. These findings may contribute to precision medicine in patients with NMIBC by classifying optimal patient subgroups and determining an appropriate therapeutic course.

## Contributors

**Seung-Woo Baek:** Data curation, Formal analysis, Investigation, and Writing. **Jeong-Yeon Mun:** Data curation and Investigation. **In-Hwan Jang:** Data curation and Investigation. **Gi-Eun Yang:** Data curation and Investigation. **Mi-So Jeong:** Data curation and Investigation. **Seon-Kyu Kim:** Data curation and Investigation. **Jong-Kill Nam:** Data curation and Investigation. **In-Sun Chu:** Investigation, Project administration, Supervision, and Writing. **Sun-Hee Leem:** Investigation, Project administration, Funding acquisition, Supervision, and Writing. All authors reviewed and approved the manuscript.

## Declaration of interests

All the authors have declared no conflicts of interests.

## Data sharing statement

The dataset generated by RNA-seq is available in the GEO public database under data series accession number GSE186043.

## Acknowledgements

## Supplementary materials

Supplementary material associated with this article can be found in the online version at doi:10.1016/j.ebiom.2022.104092.

### References

1. Siegel RL, Miller KD, Fuchs HE, Jemal A. Cancer statistics, 2021. *CA Cancer J Clin*. 2021;71:7–33.
2. Jacobs BL, Lee CT, Montie JE. Bladder cancer in 2010: how far have we come? *CA Cancer J Clin*. 2010;60:244–272.
3. Redondo-Gonzalez E, de Castro LN, Moreno-Sierra J, et al. Bladder carcinoma data with clinical risk factors and molecular markers: a cluster analysis. *Biomed Res Int*. 2015;2015: 168682.
4. Babjuk M, Bohle A, Burger M, et al. EAU guidelines on non-muscle-invasive urothelial carcinoma of the bladder: update 2016. *Eur Urol*. 2017;71:447–461.
5. Subiela JD, Rodriguez Faba O, Guerrero Ramos F, et al. Carcinoma in situ of the urinary bladder: a systematic review of current knowledge regarding detection, treatment, and outcomes. *Eur Urol Focus*. 2020;6:674–682.
6. Pfail JL, Katims AB, Alerasool P, Sfakianos JP. Immunotherapy in non-muscle-invasive bladder cancer: current status and future directions. *World J Urol*. 2020.
7. Sjodahl G, Lauss M, Lovgren K, et al. A molecular taxonomy for urothelial carcinoma. *Clin Cancer Res*. 2012;18:3377–3386.
8. Hedegaard J, Lamy P, Nordentoft I, et al. Comprehensive Transcriptional analysis of early-stage urothelial carcinoma. *Cancer Cell*. 2016;30:27–42.
9. Song BN, Kim SK, Mun JY, Choi YD, Leem SH, Chu IS. Identification of an immunotherapy-responsive molecular subtype of bladder cancer. *EBioMedicine*. 2019;50:238–245.
10. Robertson AG, Kim J, Al-Ahmadie H, et al. Comprehensive molecular characterization of muscle-invasive bladder cancer. *Cell*. 2017;171:540–556. e25.
11. Kim SK, Roh YG, Park K, et al. Expression signature defined by FOXM1-CCNB1 activation predicts disease recurrence in non-muscle-invasive bladder cancer. *Clin Cancer Res*. 2014;20:3233–3243.
12. Pardo JC, Ruiz de Porras V, Plaja A, et al. Moving towards personalized medicine in muscle-invasive bladder cancer: where are we now and where are we going? *Int J Mol Sci*. 2020;21.
13. Harvey KF, Zhang X, Thomas DM. The Hippo pathway and human cancer. *Nat Rev Cancer*. 2013;13:246–257.
14. Nguyen CDK, Yi C. YAP/TAZ signaling and resistance to cancer therapy. *Trends Cancer*. 2019;5:283–296.
15. Ooki A, Del Carmen Rodriguez Pena M, Marchionni L, et al. YAP1 and COX2 coordinately regulate urothelial cancer stem-like cells. *Cancer Res*. 2018;78:168–181.
16. Qiu D, Zhu Y, Cong Z. YAP triggers blader cancer proliferation by affecting the MAPK pathway. *Cancer Manag Res*. 2020;12:12205–12214.
17. Park HW, Kim YC, Yu B, et al. Alternative Wnt signaling activates YAP/TAZ. *Cell*. 2015;162:780–794.
18. Lee JS, Leem SH, Lee SY, et al. Expression signature of E2F1 and its associated genes predict superficial to invasive progression of bladder tumors. *J Clin Oncol*. 2010;28:2660–2667.
19. Mariathasan S, Turley SJ, Nickles D, et al. TGFbeta attenuates tumour response to PD-L1 blockade by contributing to exclusion of T cells. *Nature*. 2018;554:544–548.
20. Dobin A, Davis CA, Schlesinger F, et al. STAR: ultrafast universal RNA-seq aligner. *Bioinformatics*. 2013;29:15–21.
21. Liao Y, Smyth GK, Shi W. featureCounts: an efficient general purpose program for assigning sequence reads to genomic features. *Bioinformatics*. 2014;30:923–930.
22. Wilkerson MD, Hayes DN. ConsensusClusterPlus: a class discovery tool with confidence assessments and item tracking. *Bioinformatics*. 2010;26:1572–1573.
23. Casadei C, Dizman N, Schepisi G, et al. Targeted therapies for advanced bladder cancer: new strategies with FGFR inhibitors. *Ther Adv Med Oncol*. 2019;11: 1758835919890285.
24. Lee SR, Roh YG, Kim SK, et al. Activation of EZH2 and SUZ12 regulated by E2F1 predicts the disease progression and aggressive characteristics of bladder cancer. *Clin Cancer Res*. 2015;21:5391–5403.
25. Baek SW, Jang IH, Kim SK, Nam JK, Leem SH, Chu IS. Transcriptional profiling of advanced urothelial cancer predicts prognosis and response to immunotherapy. *Int J Mol Sci*. 2020;21.
26. Mouw KW, Goldberg MS, Konstantinopoulos PA, D'Andrea AD. DNA Damage and Repair Biomarkers of Immunotherapy Response. *Cancer Discov*. 2017;7:675–693.
27. Liu Y, He K, Hu Y, et al. YAP modulates TGF-beta1-induced simultaneous apoptosis and EMT through upregulation of the EGF receptor. *Sci Rep*. 2017;7:45523.
28. Yu M, Chen Y, Li X, et al. YAP1 contributes to NSCLC invasion and migration by promoting Slug transcription via the transcription cofactor TEAD. *Cell Death Dis*. 2018;9:464.
29. Shibue T, Weinberg RA. EMT, CSCs, and drug resistance: the mechanistic link and clinical implications. *Nat Rev Clin Oncol*. 2017;14:611–629.
30. Wang Y, Appiah-Kubi K, Wu M, et al. The platelet-derived growth factors (PDGFs) and their receptors (PDGFRs) are major players in

oncogenesis, drug resistance, and attractive oncologic targets in cancer. *Growth Factors*. 2016;34:64–71.

31 Papadopoulos N, Lennartsson J. The PDGF/PDGFR pathway as a drug target. *Mol Aspects Med*. 2018;62:75–88.

32 Neuzillet C, Tijeras-Raballand A, Cohen R, et al. Targeting the TGFbeta pathway for cancer therapy. *Pharmacol Ther*. 2015;147:22–31.

33 Kang HW, Kim YH, Jeong P, et al. Expression levels of FGFR3 as a prognostic marker for the progression of primary pT1 bladder cancer and its association with mutation status. *Oncol Lett*. 2017;14:3817–3824.

34 Thoma C. Bladder cancer: improving NMIBC risk stratification. *Nat Rev Urol*. 2018;15:138.